International Journal of Geotechnical Earthquake Engineering
Volume 14 • Issue 1

Behavior of Low Height Embankment Under Earthquake Loading

Debabrata Ghosh, Jadavpur University, India
Narayan Roy, Jadavpur University, India*
Ramendu Bikas Sahu, Jadavpur University, India

ABSTRACT

Low height embankments are widely used as road embankments for highways and rural roads in India. Sometimes, the construction of such types of embankments on soft foundation soil becomes mandatory. In addition to the problematic soft foundation soil, seismic excitation might also play a significant role in the stability of such an embankment. The present study analyses the response of a low height embankment with soft foundation soil under earthquake loading. Numerical simulations have been performed using FLAC2D program. A stiffer half-space with higher shear wave velocity (Vs) has been considered below the soft foundation soil and the earthquake loading has been applied at the bottom of this stiffer half-space. Simulation has been performed considering two different thicknesses of soft foundation soil. In addition to that, three different levels of earthquake shaking and Vs of the stiffer half-space have been considered in the analysis. Results have been presented in the form of PGA amplification, excess pore water pressure, horizontal, vertical static/seismic displacement, etc.

KEYWORDS

Embankment, Excess Pore Water Pressure, PGA, Seismic Excitation, Soft Soil

1. INTRODUCTION

Embankment is a widely used civil structure serving various purposes since a long time. It can be used as earthen dam, rock-fill dam, roadway, railway embankment etc. An embankment can be used for different purposes depending on which it may be said as low height or high embankment, steep slope or gentle slope embankment, homogeneous or composite embankment. According to the purpose of use, it gets subjected to several kind of forces and their combinations. An embankment can be subjected to the gravitational forces, sudden drawdown forces, seepage forces, seismic forces, artificial hazards etc. The dynamic analysis is comparatively new. As since the 1960 several earthquake events around the world caused damages to several major structures and the significance of the response of earthen structures under dynamic loading has become evident. In this particular study, the response of a low height embankment (roadway, railway) built over soft foundation clay followed by stiff clay

DOI: 10.4018/IJGEE.315798 *Corresponding Author

layer will be assessed and analyzed. Since last few decades, the researchers across the world have developed several analytical, empirical, semi-empirical methods to analyze the slopes or embankment under seismic condition and determined the settlement, factor of safety etc.

Terzaghi (1950) proposed the pseudo-static method with introduction of pseudo-static horizontal and vertical pseudo-acceleration in the zone of failure mass that represents the dynamic forces induced due to earthquake. This method provides FOS of the embankment but does not calculate the settlement and it is widely approximate method. Newmark (1965) hypothesized the failure mass in a slope as sliding block on an inclined plane. The permanent deformation doesn't occur as long as the seismic induced acceleration amplitude is less than the yield acceleration. By double integrating the acceleration in excess of the yield acceleration over the seismic period the permanent deformation is determined. Seed et al. (1973) developed a procedure to calculate seismic induced slope deformation from the results of linear or equivalent linear analyses. The cyclic shear stresses are calculated in each element of dynamic finite-element analysis. Deformations are then estimated as the product of the average strain potential along a vertical section through the slope and the height of that section. Makdisi and Seed (1978) used block theory and Chopra's method (1966) for calculating the permanent deformation of a slope and embankment and expressed that in form of chart. Lefebvre & Pfendler (1996) showed that the shear strength of undisturbed soft clay decreases rapidly with no initial static stress with increase in number of scale but compensated by strength mobilization associated with high strain. Cyclic resistance decreases with increase in initial static stress but cyclic degradation is less. Wartman et al. (2001) conducted a series of shaking table tests using clayey slope under two successive test motions. Accelerometer and displacement potentiometer were installed at salient points to records the behavior of the model under two successive identical earthquake motions. Egawa et. al (2004) investigated the behaviour of embankment on peat ground under seismic loading through a series of centrifuge model tests. The author studied the effects of thickness of peat ground, the height of embankments, frequency and acceleration level of the input motion. It was observed that as the frequency of input motion approaches the natural frequency, the settlement of the peat layer increased because of high acceleration response. The acceleration response increases in the central depth of the ground. The higher the initial shear modulus of the peat ground, the decline in acceleration response is more prominent. Endi Zhai et. al. (2004), analysed and compared the results of shaking induced cyclic shear stresses and permanent deformations obtained by equivalent linear and nonlinear effective-stress approach with the finite difference code FLAC. The authors analysed Stone Canyon Dam located in Los Angeles, California by both equivalent linear method and fully non-linear method. Although the total accumulated pore pressures at the end of shaking doesn't vary too much, but the shaking induced permanent deformation obtained from two methods differs significantly. For more realistic analysis, the authors used FLAC3D which resulted in maximum crest deformation. The authors also concluded that the shaking induced excess pore-water pressure and reduction of stiffness of the soil affects the dynamic response of the embankment significantly. Melo and Sharma (2004) studied the dependency of the seismic coefficient on the geometry and slope angle, characteristics of the input loading etc. They used horizontal accelerogram data recorded for Northbridge earthquake (1994) and Mohr-Coulomb constitutive model and FLAC software program for analysis. Singh and Roy (2009), studied 152 published case histories about the performance of embankment during the earthquake to correlate the crest settlement of the embankment with the major influencing factor. Authors concluded that settlements are larger when the fundamental period of the embankment is close to the dominant period of the input motions, and the crest settlement may lead up to 1 metre depending on a_y/a_{max} ratio. Parish et. al. (2009) analysed the behaviour of core and shell of an embankment subjected to seismic excitation using the Mohr-Coulomb constitutive model. Authors showed that plasticity should be included in the analysis of the embankment under seismic loading. As the plasticity may change the natural frequencies, which in turn can significantly changes the response of an embankment. Giri and Sengupta (2010) conducted a shaking table test on physical models and the results were compared with the results of numerical modelling using finite difference program. In shaking table tests, the

amplification of acceleration response is observed with an increase in the height of model slopes. The numerical analysis by FLAC, in general, modelled the crest settlements reasonably well but does not predict the heaving and outward movement at toe. Okamura and Tamamura (2011) investigated the seismic stability of embankment on soft clay and peat deposits. Authors observed the higher excess pore pressures in the saturated zone of the embankment during shaking. The crest settlement and deformation of embankment during shaking were larger for the embankment on soft clay. Jakka et al. (2011) studied the seismic slope stability of embankments constructed with pond ash. Authors concluded that the response is influenced by type of construction, in situ conditions, magnitude of dynamic loads, static and dynamic characteristics of the materials etc. similar to natural soils.

Long and Tjok (2013), analysed the earthquake liquefaction phenomenon in a submarine slope using FLAC2D. The authors used an input motion with PGA 0.48g and power spectrum of the input motion lies mostly in the lower frequency range (less than 10 Hz). The slope is found to be moved horizontally 8.5m after the completion of seismic excitation. Gordan et al. (2014) studied the dynamic behaviour of short embankment on soft soil. For this purpose, the authors carried out numerical analysis using ANSYS13 program with the FE method. Simulated models were shaken by earthquake loading with specified PGA and time. Then the authors compared results on plane strain analysis based on the modular ratio between embankment and foundation. Paulus P. Rahardjo (2014) discussed some case histories of excavation and embankment failures in Indonasia and also discussed some aspects of analytical and empirical methods of geotechnical analysis. The main cause of bearing capacity failure of the foundation soil is excess pore pressure generation during the cyclic loading. Another important reason of the failure is that the embankment is much stiffer. Cracks are found to be developed upon sufficient amount of movement and due to the significant difference in the stiffness between the soil of embankment and foundation soil. Cappa et al. (2015) studied the settlement and pore pressure generation in the soft peaty soil under embankment during cyclic loading via centrifuge testing. The study emphasises on the post cyclic behaviour of peaty soil and its immediate, primary and secondary settlement. Excess pore pressures developed in the peat during shaking and the secondary compression settlement rate were observed to increase due to cyclic straining. This suggests a strong potential hazard for accelerated long term crest settlements (i.e., reduction of freeboard) following seismic events, in particular for areas with minimal pre-earthquake secondary settlement rates. Yu-liang et. al. (2016), carried out a numerical case study on the behaviour of embankment under the influence of seismic loading using FLAC3D code and the authors verified the numerical results with shaking table tests. The study includes horizontal and vertical acceleration response and dynamic displacement response. The magnification is more near embankment slope than in the internal portion of the embankment. The author also found that with the increase in peak acceleration of input motion, the magnification shows a decreasing trend. The vertical acceleration response is found to be less sensitive to the input motion than the horizontal acceleration response. Bandyopadhyay et. al. (2017) studied the Apsara dam to predict its response during seismic excitation using 2D plane strain finite element analysis. They used a real earthquake compatible with response spectrum to evaluate the earthquake induce deformation. The deformation was also calculated with the help of different popular procedure like Seed and Makdisi's method, Jansen's method and Swaisgood's method, Newmark's double integration method. The Seed and Maksidi method yield the largest lateral displacement and Jansesn's method predicts the largest crest settlement. Sitharam and Hegde (2019) studied the probabilistic seismic slope stability analysis of rock fill tailing dam using Monte Carlo simulation method. The cohesion (c), angle of internal friction and earthquake acceleration were taken as the random variable. The probability of failure value was obtained to be less than 8%. Bardhan and Samui (2022) presented a study considering the application of different Artificial Intelligence Techniques in slope stability analysis.

From the previous studies, it is quite evident that more rigorous analyses considering other aspects of earthquake shaking should be considered in future studies. In this paper, the performance of a low height embankment on soft clay followed by a stiff clay under dynamic loading is studied. The input motion of Loma Prieta Earthquake is scaled to different intensity level in order to study the effect of

different earthquake shaking level on embankment response. The thickness of soft clay layer and shear wave velocity of stiff clay layer have also been varied in the analysis for the purpose of depicting a picture of how these parameters influence the seismic response of an embankment. The results are expressed in the form of different parameters like amplification, settlement, excess pore water pressure etc.

2. METHODOLOGY

2.1. Model Description

An embankment model is developed in the finite difference software FLAC2D (v.7.0). The embankment as well as its foundation is assumed to be made of clayey soil. Figure1 presents the schematic diagram of the embankment model considered in the present study. The embankment-foundation system shows that the embankment is constructed on a soft foundation soil which is again underlain by a stiffer half-space made of stiff clayey soil.

Table1 presents the engineering properties of the embankment and its foundation soil. The earthquake motion is applied at the base of the stiffer soil of the model. The Mohr-Coulomb model which is a simple plastic constitutive model, is adopted to define the stress-strain relationship of the soil material, and while subjected to dynamic loading, two modes of analysis are conducted; one considering no damping and the other with hysteresis damping to study the influence of damping. The seismic excitation is applied at the base of the model i.e., at RL -50.0. The water table is considered at the bottom of embankment (RL 0.0). In all cases, no seepage conditions through the embankment have been considered.

The numerical analysis began from prior embankment construction stage. After the embankment construction, due to the additional embankment loading some instantaneous settlement occurs. After the construction of the embankment, no dissipation of pore water pressure allowed as this may increase the strength of the foundation soil. So as to consider the more vulnerable scenario, the input ground motion has been applied before any consolidation takes place. Mohr-Coulomb model does not account the degradation of shear modulus due to reversible/cyclic loading. In damped analysis, the Mohr-Coulomb constitutive model is linked with hysteresis damping to simulate strain-dependent modulus degradation. The damping is also a function of permanent strain. To model the strain dependent shear modulus and damping behaviour, the defaults curves associated with modulus reduction and damping characteristics available for clayey soil have been used in the analysis. At larger strain level,

Figure 1.
Schematic Diagram of the embankment-foundation model (not to scale) considered in the study

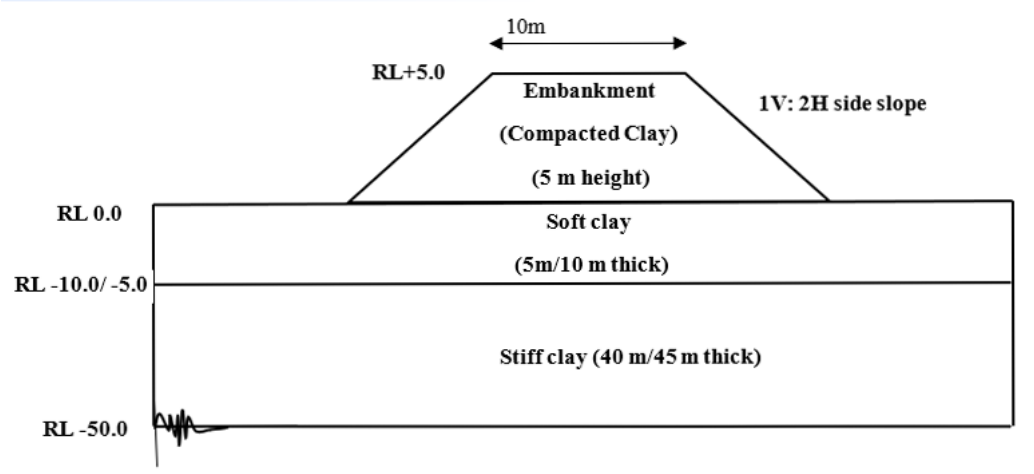

Table 1.
Soil Properties of the construction materials of embankment and its foundation

Properties	Unit	Half-Space (Stiff Clay layer)	Foundation Soil (Soft Clay layer)	Embankment (Compacted Clay)
Density	Kg/cum	2000	1700	1900
Cohesion	Pa	100000(for V_s= 800) 80000 (for V_s=500) 70000 (for V_s=300)	32	40
Frictional Angle	Degree	0	0	20
Poisson's Ratio		0.35	0.35	0.35
Shear Velocity (V_s)	m/sec	800/500/300(for different cases)	100	150
porosity		0.3	0.4	0.35
Initial Shear Modulus (G_{max})	MPa	180 (for V_s=300) 500 (for V_s=500) 1280 (for V_s=800)	17	42.75

the soil plasticity and damping can severely affect the embankment response to the earthquake. In the embankment like structure which is used for transportation purpose, the degree of crest settlement is important to determine the serviceability of the embankment after earthquake. The soil properties and geometry are chosen in such a way that under static condition the embankment is well stable. The Side-slopes are kept 2H:1V and the static FOS is kept over 1.50 with potential base failure.

2.2. Boundary Conditions

In the static analysis phase, the normal boundary condition for soil structures is applied to the model. Along the base, the fixed boundary is assigned and the roller boundary is assigned at the sides of the model. Top surface of the model is kept free. After completion of static analysis, the dynamic loading is applied. Before the application of dynamic loading, proper boundaries are to be applied to the model. The choices of boundaries depend on the mode of application of the input motion. In this study, the input motion is given at the model base (RL -50.0+) in the shear stress waveform. The "quiet" boundary criteria are applied along the base of the model (along RL-50.0) and the "free field boundary" criteria are applied along both the sides of the model (from RL -50.0 to RL 0.0 both sides). The top surface is kept free i.e., shear stress on the top surface is zero.

Figure 2 presents the schematic of the model along with assigned boundaries along the base and sides of the model. The seismic wave propagating upward should not get distorted due to the presence of quiet boundary at the base and free field boundary at the sides.

2.3. Input Motion

The embankment is subjected to the seismic loading representative of the Loma Prieta earthquake in California. The original record shows a peak acceleration of 3.7 m/s^2 and total acceleration time record is of 40 seconds approximately. For analysis, to investigate the effects of peak acceleration on the embankment, the seismic record is scaled in the acceleration axis to the PGA values of 0.07g, 0.15g and 0.25g. Now the input loading is applied in the form of shear stress wave-time history, so the stress-history is derived from the acceleration-time history. The acceleration time history is initially converted to the velocity time history, and then shear stress wave -time history is derived. The relationship between magnitude of stress and particle velocity is shown in the following equation

$$l\tilde{A}l = 2\rho C_s V_s \quad (1)$$

Figure 2.
Boundary conditions assigned to the model

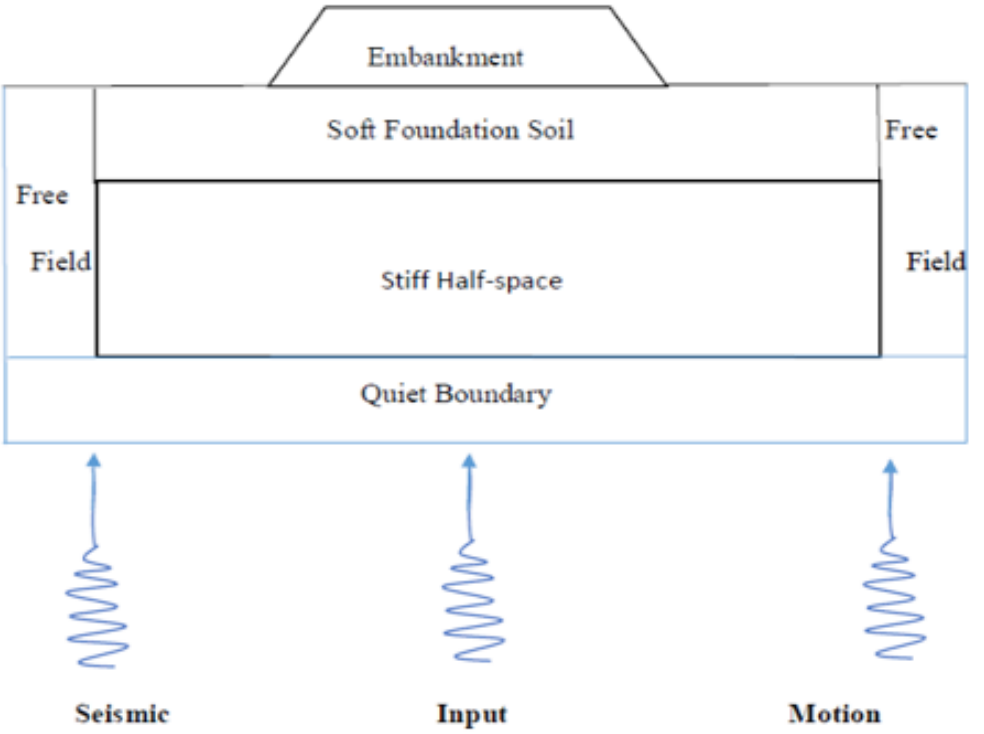

σ = shear stress; ρ = mass density of material; C_s = Shear wave velocity in the medium; V_s is input particle velocity i.e., the velocity-time history derived from the acceleration time history. Figure 3 shows the adopted acceleration time history (Fig. 3a) along with the power spectra (Fig. 3b) of Loma Prieta earthquake. The motion is having a PGA of 0.37g. The power spectra clearly depict the significant power associated with 0.5Hz to 5Hz. Now, in order to simulate the embankment behaviour for different level of induced strain, the original input motion is scaled to three different PGA values: 0.07g, 0.15g and 0.25g. Figure 4 represents the scaled input motion of Loma Prieta earthquake.

2.4. Mesh Generation

After assigning the material and its associated engineering properties for each layer along with the embankment, the next step is the generation of mesh in the model to divide the models into small elements which are needed for subsequent analyses under different loading conditions. Now, for accurate results, the mesh sizes need to be as fine as possible. But with the fine meshing, the calculation time increases significantly and sometimes, some numerical errors may arise. So, a balance should be maintained in choosing the mesh element size and calculation time. Among the three options available with the software, the fine mesh option should provide more accurate results. But, in this study, the dynamic (seismic) loading is also associated with the analysis. So, only the fine meshing cannot guarantee an accurate analysis. The element sizes are also to be checked in association with the frequency content of the input acceleration time history. From the plot of the power spectrum (Fig. 3b) of the acceleration time history, the maximum frequency of interest can be taken as 10Hz. So, 10 Hz frequency can be taken as the guiding frequency for fixing the maximum mesh size. Kuhlemeyer and Lysmer (1973) showed that for an accurate representation of the wave transmission through a

Figure 3.
Loma Prieta Earthquake (a) Recorded acceleration time history (b) Power Spectrum

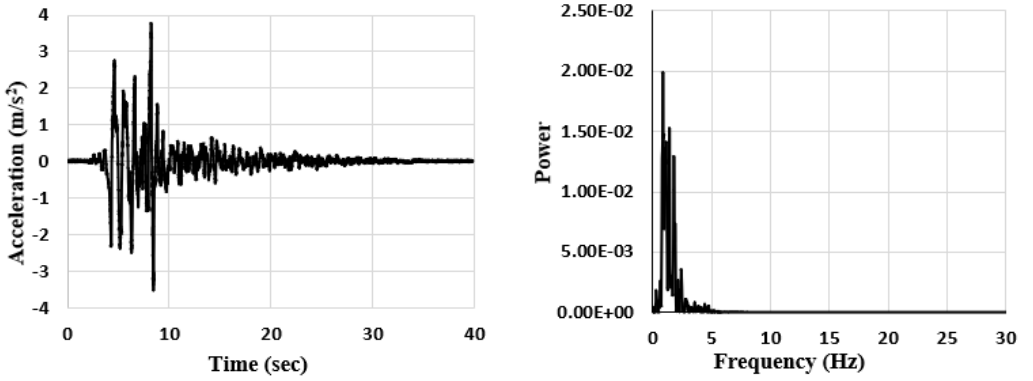

Figure 4.
Loma Prieta Earthquake scaled to (a) 0.07g (0.69 m/s²), (b) 0.15g (1.47 m/s²) and (c) 0.25g (2.45 m/s²)

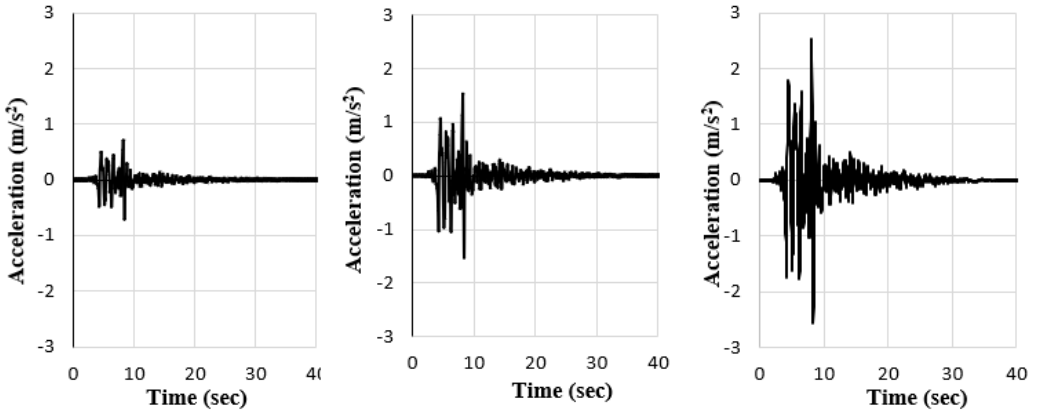

soil model, the spatial element size, Δl, must be smaller than approximately one-tenth to one-eighth of the wavelength associated with the highest significant frequency. The mesh size is decided based on maximum frequency content of the input motion and least shear velocity of the material. Now, the minimum shear velocity belongs to the soft clay foundation layer and the velocity is ~100 m/sec. So, the minimum wavelength that is considered in the analysis can be calculated as:

$$\text{wavelength } (\lambda) = \frac{\text{shear velocity}}{\text{significant maximum frequency}} = = \frac{100}{10} \text{ m} = 10 \text{ m} \quad (2)$$

Maximum element size(Δl) is taken as one-tenth of the wavelength i.e. 0.1x10 m =1m. The element size can be further reduced to get finer results but, in that case, the computation time will increase significantly without any significant increase in the accuracy of the results. So, the mesh size is fixed as 1m x 1m, and in case of triangular elements, the maximum size of the sides is 1.0 m. This mesh size ensures that the maximum frequency that can be simulated accurately is 10 Hz. Figure 5 shows the generated mesh following the above adopted criteria.

Figure 5.
Embankment model shown with mesh generated elements

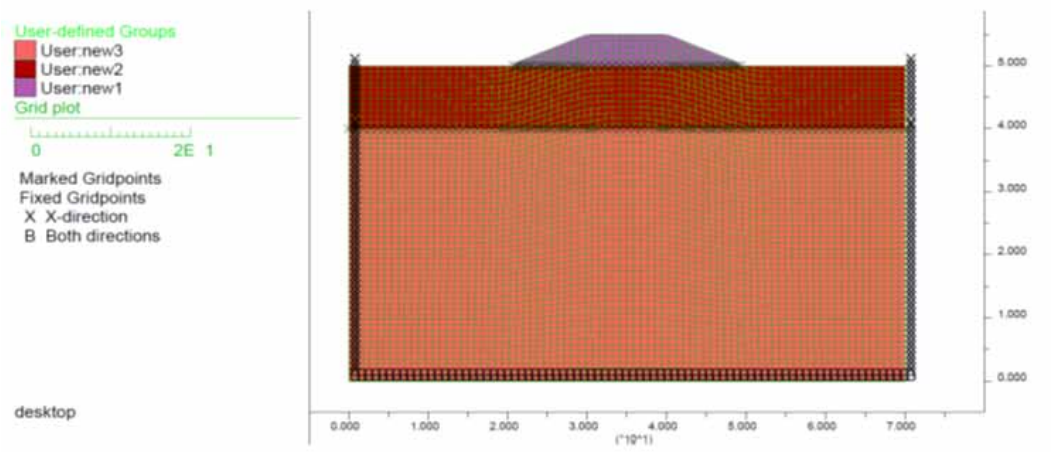

2.5. Combinations of Study

A small height embankment of height 5m has been considered in the analysis. The height of the embankment has been taken quite small as the study is strictly restricted for low height embankments. Two different soft layer thicknesses of 5m and 10m are chosen for each height of the embankment. In addition to these, three different shear wave velocities of the stiffer half-space have been considered for each case with a total 6 different combinations. Again, each combination is analysed for three different input ground motion, which leads to a total 18 different combinations of study. Table 2 describes the details of the combinations of models analysed in this study. The variation of stiffer half-space is considered in order to study how the half-space shear wave velocity further influences the wave propagation phenomena. In order to consider different level of shaking, the original input motion of Loma Prieta Earthquake is scaled to three different PGA values. It is a well-known fact that level of shaking significantly influences the behavior of a soil by degrading the shear modulus and increasing the damping ratio. So, to take into account the complete behavior of soil covering a large range of induced strain, different level of shaking has been considered in this study.

3. RESULTS AND DISCUSSIONS

3.1 Static Analysis

As the study is mainly concentrated for low height embankment, the construction is assumed to be completed in one stage, and the instantaneous settlement is calculated for all the models. The consolidation settlement is not taken into consideration as the completion of consolidation would take years for dissipating the excess pore water pressure. After the completion of consolidation, the stability and strength of the embankment foundation system will increase and make it well resistant to the earthquake loading. In order to simulate the study for worse condition, the dynamic loading is applied immediately after the construction of the embankment without allowing any dissipation of excess pore water pressure (PWP). The seepage through embankment has also been ignored here as the embankment considered is a typical small height road/rail embankment, and seepage is not an issue for such type of structure. So, in the static analysis, the instantaneous settlement is measured and the static FOS is calculated.

Table 2.
Geometric Specifications of the Embankment Model with Foundation Soil

Model Name	Embankment Height (m)	Soft layer Thickness	Side slope	Soft layer cohesion (kPa)	Half-space velocity (m/s)	Half-space Cohesion (Pa)
MOD1	5.0	10.0	2H:1V	32	300	70000
MOD2	5.0	10.0	2H:1V	32	500	80000
MOD3	5.0	10.0	2H:1V	32	800	100000
MOD4	5.0	5.0	2H:1V	32	300	70000
MOD5	5.0	5.0	2H:1V	32	500	80000
MOD6	5.0	5.0	2H:1V	32	800	100000

Figure 6(a) presents the contour diagram of the developed PWP of foundation soil before the embankment is placed. It varies from the range of 0 Pa at the top of foundation soil and 4.5 x 10^5 Pa at the bottom of the model increasing downward. After this, the embankment loading is placed on foundation soil. An example of the pore pressure increments after embankment loading for MOD1 is shown in Fig. 6b. This contour diagram will be the same for MOD1, MOD2, MOD3, MOD4, MOD5, MOD6 with embankment height 5m.

The static stability of the embankment is analysed after the construction of the embankment and is expressed in terms of the static factor of safety. The factor of safety for all the 6 models along with instantaneous vertical settlement is tabulated in Table 3. The typical pattern of the failure of all models is a base failure. As the slope (2H: 1V) considered in the analysis is gentle and the embankment is constructed on soft foundation clay, so the base failure pattern is justified. The typical base failure pattern is evident from the accumulated strain contour shown in Fig.7. These figures show the shear strain contours of MOD1 (Fig. 7a) and MOD4 (Fig. 7b), which clearly depict the potential failure surface as a probable base failure pattern. Maximum shear strain increment lies in the soft foundation soil and embankment soil. Shear strain increments in the stiff clay layer below the soft layer is not significant. The interface of the soft foundation layer and stiff clay layer is almost tangential to the maximum strain contour. Maximum shear strain increment is confined to the soft layer and embankment portion.

The Factor of Safety of all the considered models is shown in in Table 3. The variation of factor of safety (FoS) depicts that the main deciding factor in the FoS variation is the thickness of the soft clayey foundation layer. For the models, MOD1, MOD2 and MOD3, the soft layer thickness is 10.0 m and for rest of the models, i.e., MOD4, MOD5, MOD6 the thickness of the soft layer is 5.0 m. So, for the first three mentioned models, the factor of safety is 1.67 and for rest three models, the factor of safety is 1.80. So, this clearly depicts that as the thickness of the soft foundation soil layer increases the static factor of safety reduces, on the other hand, for lower thickness of soft foundation soil layer, a higher factor of safety is obtained.

The instantaneous settlement in terms of the vertical downward settlement of the middle of the embankment crest portion is studied and the same is tabulated in Table 3. The settlement contours suggest that the settlement primarily confined in the soft layer and embankment portion. The deformation is negligible in stiff clay portion. From the table, it can be observed that again the thickness of the soft layer influences the instantaneous settlement significantly. Like for MOD1, MOD2 and MOD3 the thickness of the soft layer is 10 m and for these models, settlement values lie between 0.0135 m to 0.016 m range. In case of MOD4, MOD5 and MOD6, where embankment height and the slope are similar like previous three cases but the soft layer thickness is 5 m (half of the previous ones), and the settlement values ranges from 0.0045 m to 0.007 mm. One more observation can be made from the table that when the half-space velocity and cohesion of half-space layer increase the settlements reduces. So, the effect of half-space strength is clearly visible here. Now, after this stage of static stability the dynamic loading is applied to the models and dynamic analysis is performed.

Figure 6.
Pore pressure distribution (a) before applying embankment loading; (b) after applying embankment loading

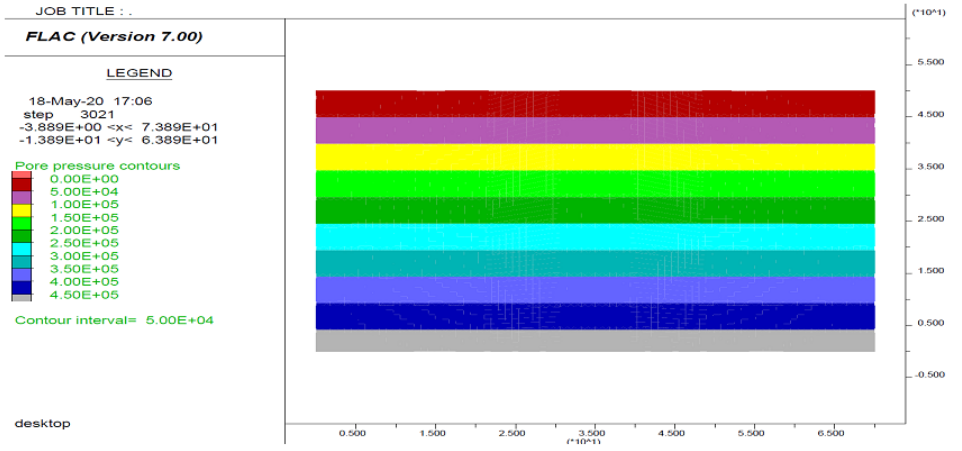

(a)

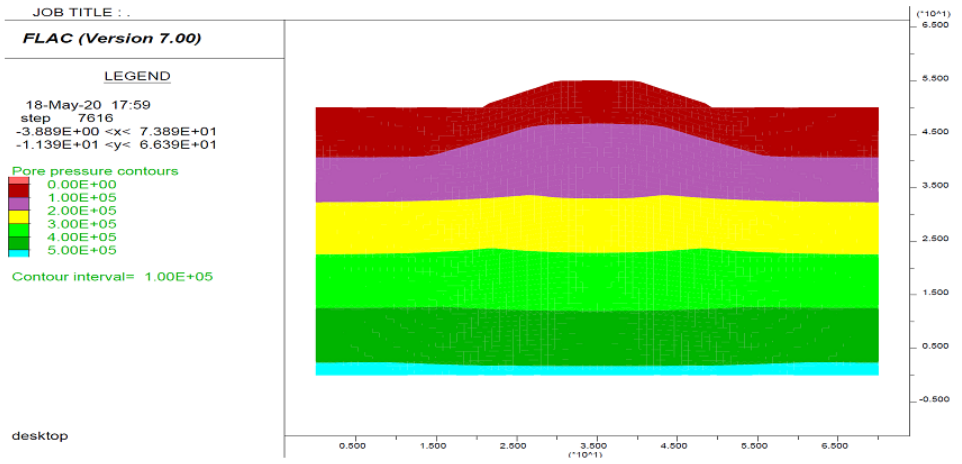

(b)

3.2. Dynamic Analysis

3.2.1 Acceleration Amplification

During the simulation using dynamic loading, the results of various parameters are studied like crest amplification, displacement (vertical, horizontal), pore water pressure etc. From the analysis and interpretation of the results monitored throughout the excitation time and thereafter, the dynamic response of the models is evaluated. When shear waves or seismic shear waves travel from one soil medium to another soil medium, the quantities like acceleration amplitude or velocity amplitude etc. gets modified and its frequency content may also get modified depending upon the properties of the soil medium and frequency content and amplitude of the input ground motion. The dynamic analysis is conducted both in damped and undamped condition. It is also observed that with the increase in input PGA value, the amplification gets decreased and it is maximum in case of PGA value of 0.07g and minimum in case of PGA of 0.25g. Figure 8 depicts the amplification values at the middle of the

Figure 7.
Shear Strain contour for embankment loading (a) MOD1 and (b) MOD4

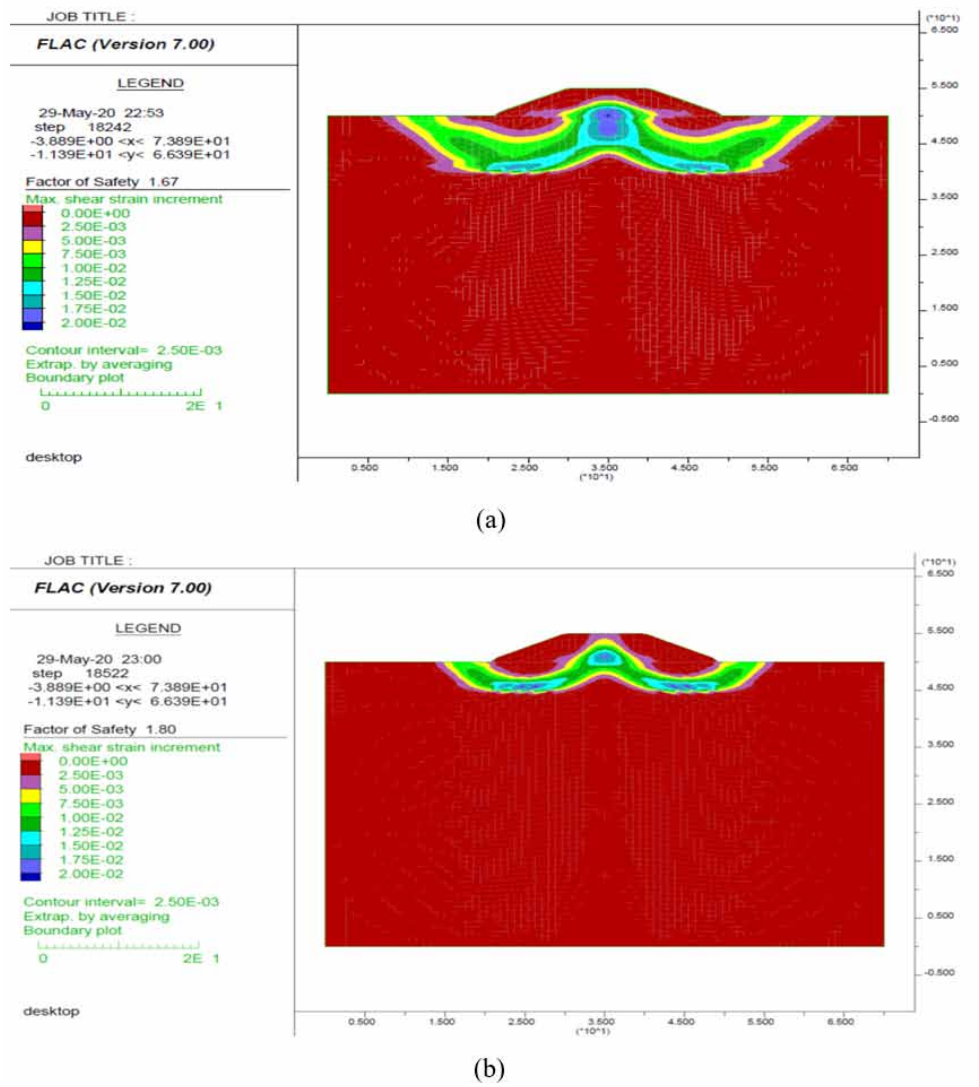

Table 3.
Instantaneous Vertical settlement of middle crest (static) and static FOS of all Model

Sl No	Model Name	Middle crest instantaneous settlement (m)	Static Factor of Safety
1	MOD1	0.0160	1.67
2	MOD2	0.0140	1.67
3	MOD3	0.0135	1.67
4	MOD4	0.0070	1.80
5	MOD5	0.0050	1.80
6	MOD6	0.0045	1.80

crest of the embankment for all the models. Fig. 8a shows the amplification variation for different PGAs and half-space velocities when the soft layer thickness is 10m, whereas Fig. 8b presents the results for the soft layer thickness of 5m. The figures clearly depict that as the PGA of the input motion increases, the crest amplification also increases with a maximum value of ~3. Table 4 presents the amplification values for all the considered cases of analysis.

Figure 8.
Amplification at the middle of the crest of the embankment for a soft layer thickness of (a) 10m and (b) 5m

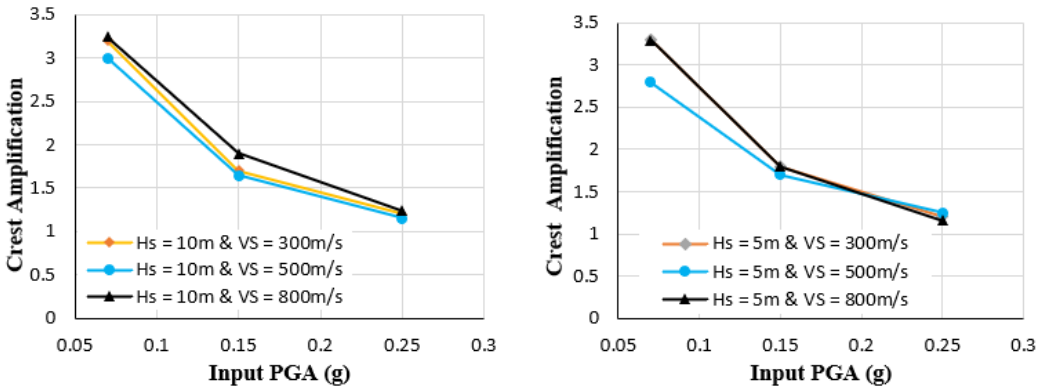

Table 4.
Horizontal Acceleration amplification between base of model and embankment crest for all models

Model	Input PGA	Amplification
MOD1	0.07g	3.2
	0.15g	1.7
	0.25g	1.2
MOD2	0.07g	3
	0.15g	1.65
	0.25g	1.15
MOD3	0.07g	3.25
	0.15g	1.9
	0.25g	1.24
MOD4	0.07g	3.3
	0.15g	1.8
	0.25g	1.2
MOD5	0.07g	2.8
	0.15g	1.7
	0.25g	1.25
MOD6	0.07g	3.3
	0.15g	1.8
	0.25g	1.16

3.2.2 Vertical Settlement

The most significant damage caused by an earthquake associated with the embankment is the vertical settlement of crest because after earthquake, serviceability of an embankment depends upon it. The stiff layer is least affected in terms of settlement due to seismic excitation. The major portion of vertical settlement is observed in soft clay layer and embankment portion. Again, the crest settlement depends on PGA, soft layer thickness and mode of analysis (damped or undamped). The middle portion and its nearby region at top of the embankment shows maximum settlement for a given PGA. The settlement of the middle point of the crest is monitored for all the models and is tabulated in the Table 5.

The vertical settlement is found more in case of damped analysis due to the strain dependent modulus degradation and damping variation except for some cases with low PGA input motions. In case of low PGA input motions, amplification is more in undamped case due to lesser role of modulus degradation and damping. For example, in case of MOD2 and MOD3 when analyzed using the input motion with PGA 0.07g, the higher vertical crest settlement is observed for undamped condition. The settlements mainly depend upon the thickness of soft soil layer. Table 5 presents the obtained values of crest settlement for different considered cases with undamped and damped conditions.

In Figure 9, the vertical settlements are plotted against PGA under damped and undamped condition. Interestingly, at lower PGA (0.07g) the MOD1 (Vs = 300m/s) shows maximum settlement but at higher PGA the MOD3 (Vs=800 m/s) shows maximum settlement. Figure 10 presents the vertical crest settlement with PGA values for different half-space velocities with soft layer thickness of 5m. The nature of variations is little different from the previous case with 10m soft layer thickness. Here, with the increase in half-space velocities lower crest settlements are found at all the PGA values. So, soft layer thickness may play an important role in embankment settlement.

Table 5.
Vertical Settlement at the middle point of the crest for all models in damped condition

Model	Input PGA	Mid-point of crest vertical settlement(m)	
		(Undamped)	(Damped)
MOD1	0.07g	0.096	0.103
	0.15g	0.140	0.152
	0.25g	0.175	0.190
MOD2	0.07g	0.080	0.075
	0.15g	0.132	0.140
	0.25g	0.187	0.200
MOD3	0.07g	0.071	0.055
	0.15g	0.150	0.155
	0.25g	0.225	0.250
MOD4	0.07g	0.026	0.030
	0.15g	0.039	0.050
	0.25g	0.052	0.070
MOD5	0.07g	0.011	0.014
	0.15g	0.022	0.025
	0.25g	0.034	0.038
MOD6	0.07g	0.006	0.007
	0.15g	0.015	0.017
	0.25g	0.030	0.034

Figure 9.
Vertical Settlement vs PGA for undamped and damped condition (HS = Soft Layer thickness, Vs = Shear velocity of bottom most stiff layer) for MOD1 to 3

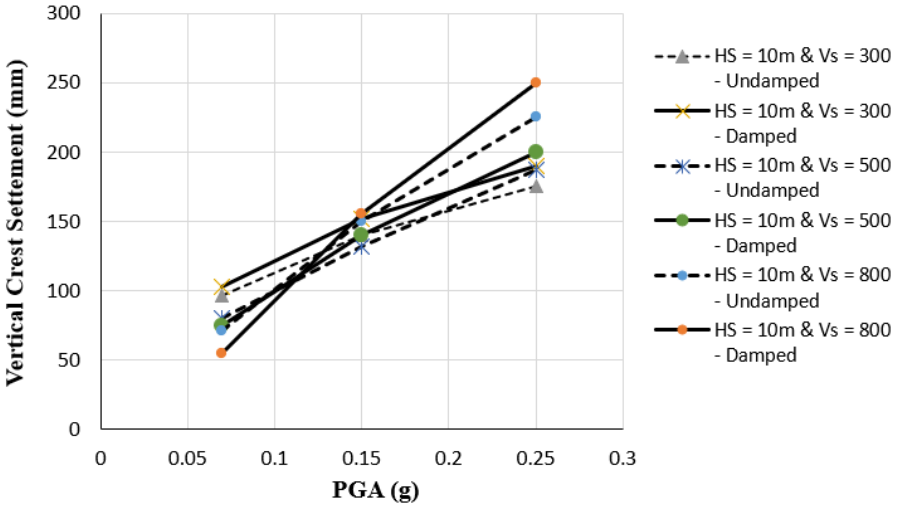

Figure 10.
Vertical Settlement vs PGA for undamped and damped condition (HS = Soft Layer thickness, Vs = Shear velocity of bottom most stiff layer) for MOD4 to 6

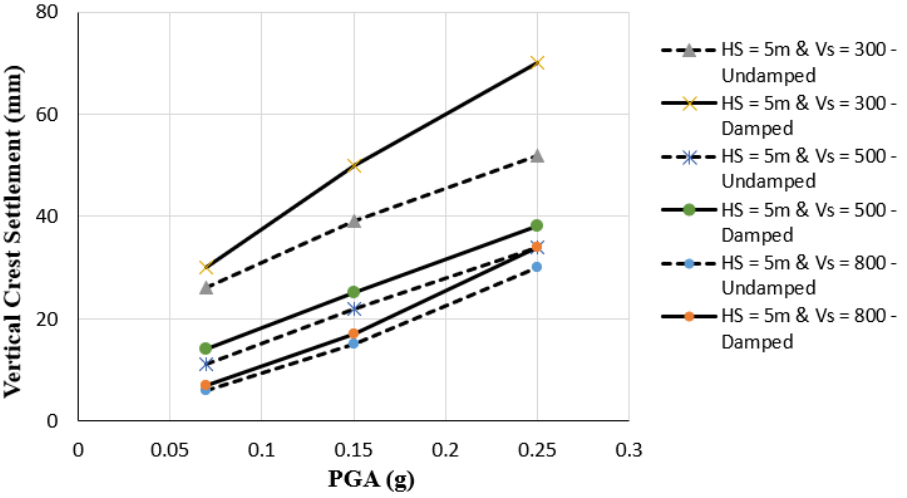

Figure 11 shows the vertical settlement contours of MOD1 and MOD4 for three different PGA input motion. From the figure, it is evident that the major vertical settlement is restricted in the embankment portion and the soft layer portion while the bottom-most stiff layer is least affected in terms of vertical settlement and this pattern is observed in all the analyzed models. The vertical settlements are mainly affected by the soft layer thickness and input motion PGA. The shear wave velocity of bottom layer also causes moderate variation in vertical settlement in an otherwise similar model. For better understanding, the variation of vertical settlement at middle of the embankment crest during the dynamic loading is shown in Figure 12. As the frequency content of all the three

Figure 11.
Vertical settlement Contours for MOD1, MOD4 for PGA 0.07g, 0.15g, 0.25g under damped condition

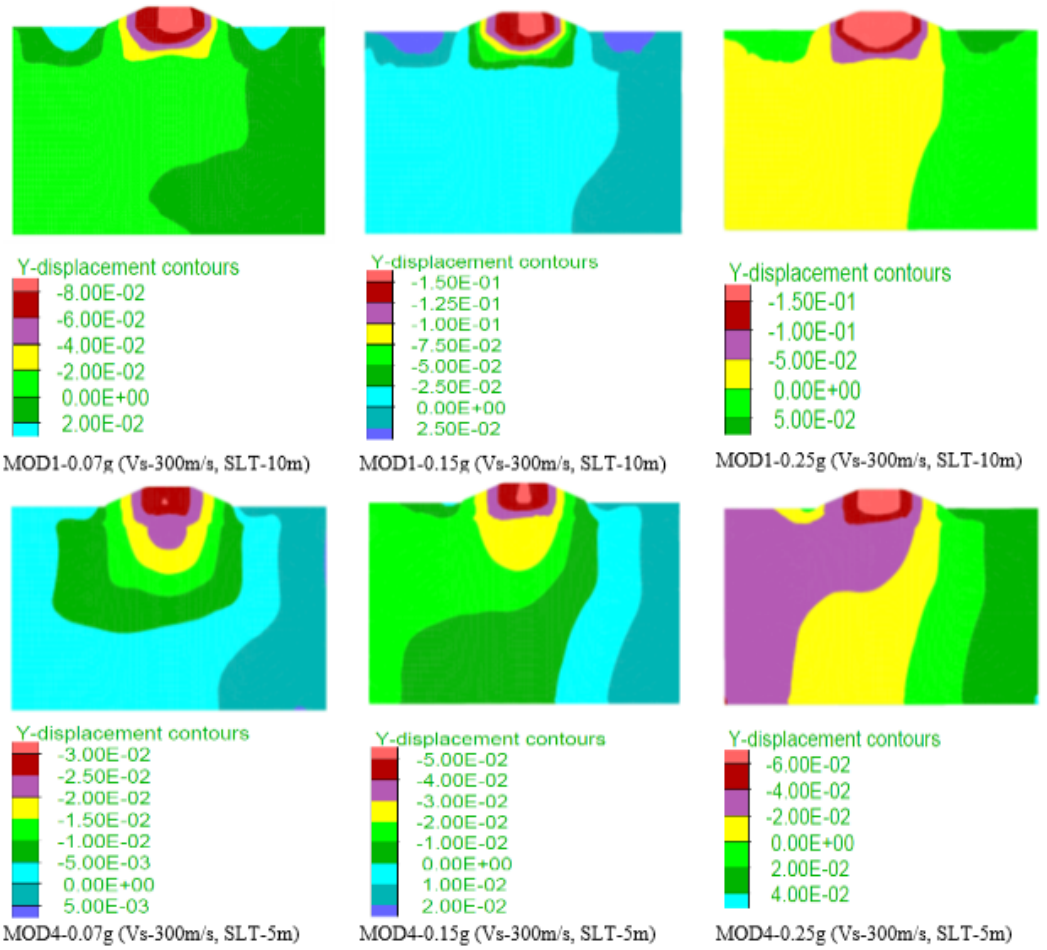

input PGA is not changed and just the peak values are changed, the displacement-time history exhibits quite similar pattern but with different maximum permanent vertical settlement increasing with increasing input PGA. The major permanent vertical settlement happens within 10 second of load application within which the major acceleration amplitude content lies. So, the intensity of shaking and the duration of significant shaking amplitudes are significantly affecting the settlement behavior of the embankment. Along with this, it is needless to say that the thickness of the soft foundation layer below embankment will also play a role here.

3.2.3 Horizontal Displacement

The lateral displacement of embankment can also affect the serviceability of an embankment. The horizontal displacement is found to be affected by input PGA and thickness of the soft layer. Interestingly, the soft foundation layer below the toe of the embankment and its neighbor regions are found to get most affected by the earthquake loading. At the crest region, the results show that the horizontal displacement is less than the soft layer portion. The soil material gets displaced at both the sides but majorly to the left side of the embankment. With the increase in input PGA from 0.07g to 0.15g to 0.25g the maximum horizontal displacement increases from 0.085 m to 0.170 m to 0.275 m at the middle of soft layer for

Figure 12.
Settlement-time history (damped Condition) of (a) MOD1 and (b) MOD4

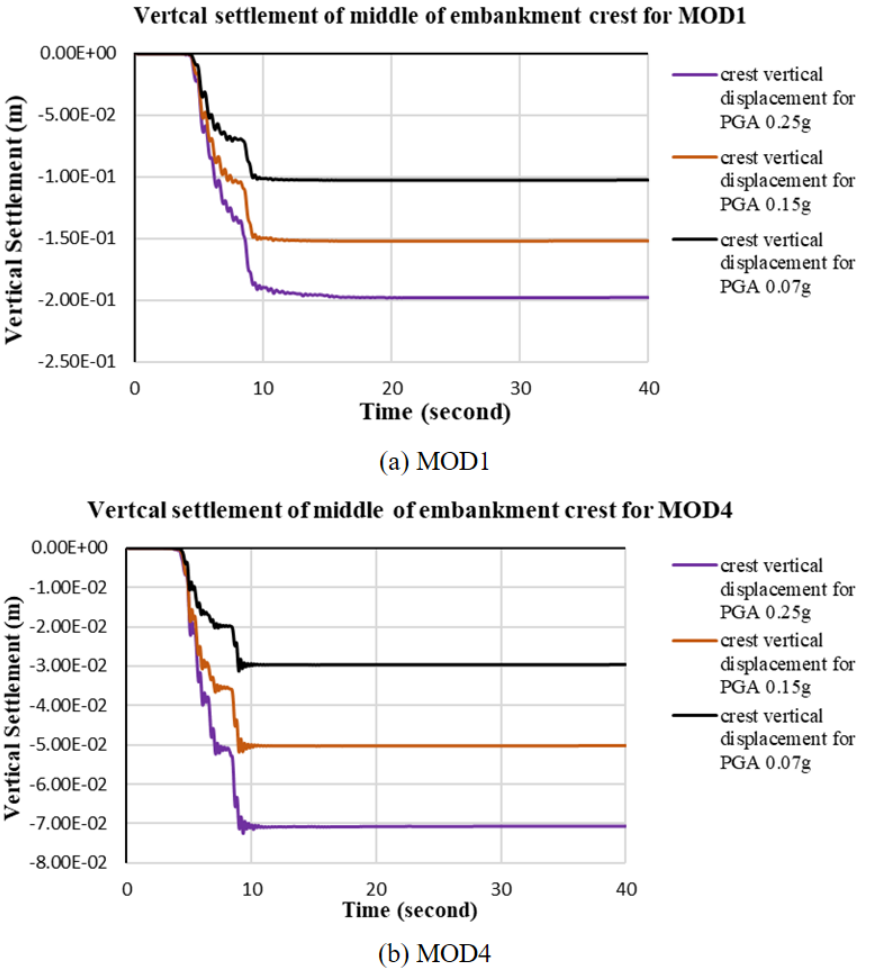

soft layer thickness of 10m (MOD1). For soft layer thickness of 5m, horizontal displacement increases from 0.020 m to 0.080 m to 0.158 m for same increase in input motion PGA (MOD4). So, the effect of thickness of soft foundation layer is quite evident here. Like MOD4 and MOD1 are identical in all parameters except the soft layer thickness. For MOD4, soft layer thickness is 5m and for MOD1, soft layer thickness is 10m. If the final horizontal displacements at the middle of soft layer is compared, the results show that the displacement increases from 0.020 m to 0.085 m (for PGA 0.07g; increase 325%), 0.080 m to 0.170 m (for PGA 0.15g; increase 112%) and 0.158 m to 0.275 m (for PGA 0.25g; 74%) with an increase in soft layer thickness of 5m. The middle portion of the embankment is relatively less displaced and the soft layer below toe is maximum displaced.

Figure 13 shows the contour diagram for permanent horizontal displacement after the application of dynamic load for MOD1 (Soft layer thickness= 10m) and MOD4 (Soft layer thickness = 5m). For the figures, it is quite evident that with the increase in soft layer thickness, the affected regions due to horizontal displacement spread more.

Similar types of horizontal displacement pattern are observed for all the models and all PGA combinations due to same dominant frequency range of the input motions. The displacement-time histories

shown in Figure 14 exhibits the variation of horizontal displacement at different points within the model MOD1 and MOD4. It is interesting that the maximum instantaneous displacements are often different from the final permanent horizontal displacement and this is not similar to vertical settlement history with time. Final permanent displacement is found to increase with increase in the PGA of input motion and with increase in soft layer thickness. The maximum and final permanent displacements of different points in the soft foundation layer are tabulated in Table 6 for MOD1 and MOD4 for different input motions.

Figure 15 shows the plot between Horizontal displacements at left toe vs input PGA at base of model for MOD1 to 6. Plots show that the pattern of the plots depends on the soft layer thickness below embankment and PGA of the input motions. For 10m soft layer thickness, the horizontal displacements get reversed at higher input PGA values with the increase in stiff layer velocity, whereas, for 5m soft layer thickness, horizontal displacements get reduced with the increase in half-space velocity for all the considered PGA values.

3.2.4 Pore Pressure

As seismic input is given to a model, the pore pressure tends to increase causing excess pore water pressure and it leads to a decrease in effective stress in general. Pore pressure at different parts of the model changes with the variation of the dynamic loading for a period of 40 second. After the full load application period gets over, value of pore pressure at a point in excess of the pore pressure

Figure 13.
Horizontal displacement contour of MOD1 & MOD4 for different PGA

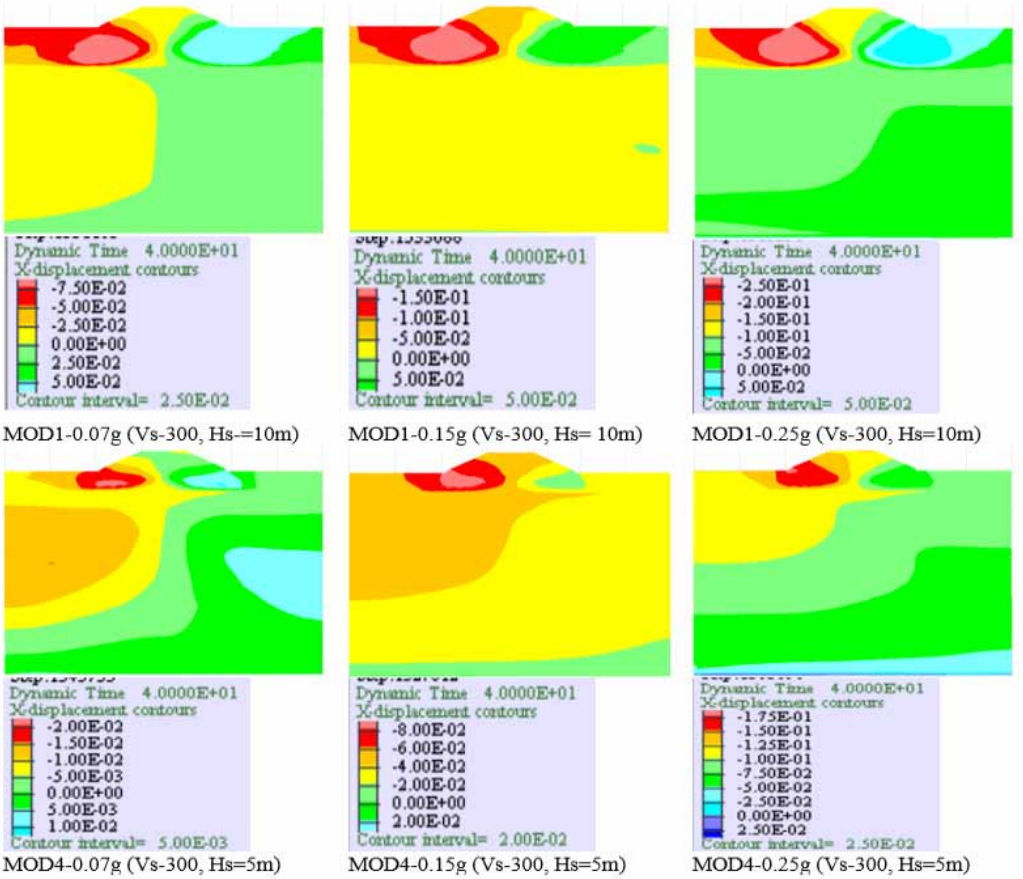

Figure 14.
Horizontal Displacement (in m) history at soft layers on vertical line through left toe (at top, mid and bottom of soft layer) for PGA of (a) 0.07g, (b) 0.15g and (c) 0.25g

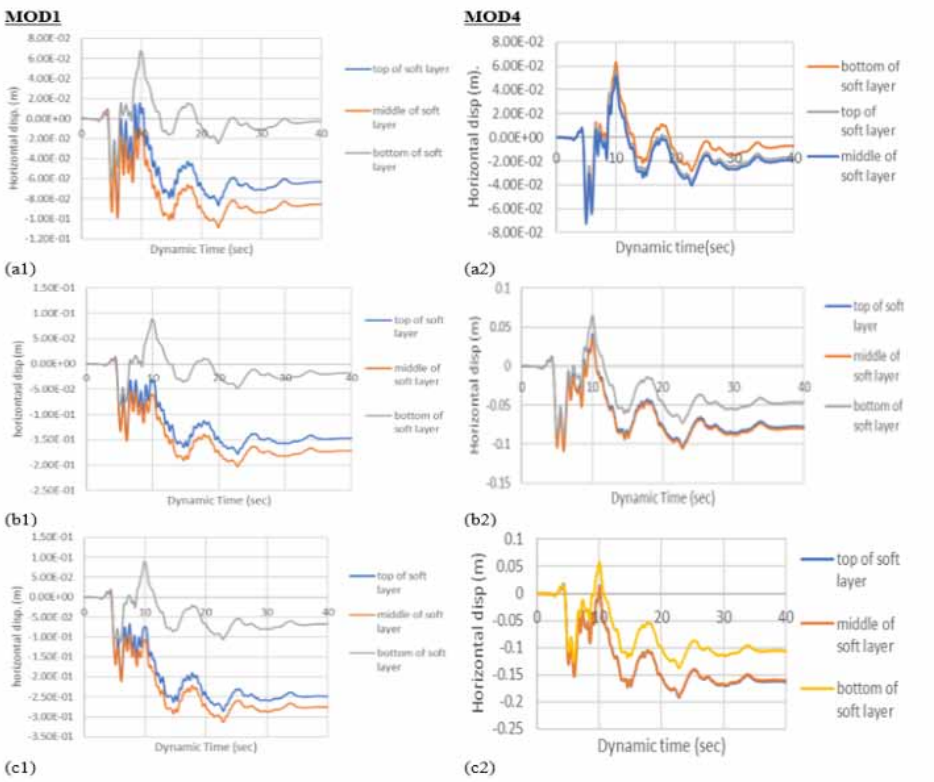

Figure 15.
Left toe horizontal displacement vs PGA (damped Condition) for soft layer thickness (a) 10m (MOD1 to 3) and (b) 5m (MOD4 to 6)

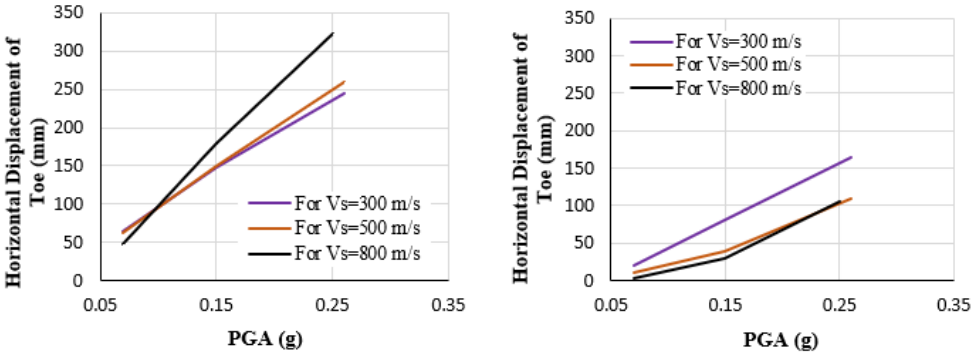

prior to the application of seismic loading is termed as the excess pore water pressure generated due to seismic loading. Figure 16 shows the effect of dynamic loading in terms of pore pressure variation for MOD1 with input PGA of 0.25g under damped condition. The figure presents the pore pressure contour before the dynamic loading (fig.16a), after the dynamic loading (fig. 16b) and excess pore

Table 6.
Maximum instantaneous and Final horizontal displacement due to seismic loading in MOD1 and MOD4 (under damped condition)

Model Name	Input PGA	Maximum horizontal displacement (m) in soft layer (Mid Vertical line)			Final Permanent displacement (m) in soft layer (Mid Vertical line)		
		bottom	Mid	Top	Bottom	Mid	Top
MOD1	0.07g	0.065	0.107	0.083	0.04	0.085	0.063
	0.15g	0.085	0.202	0.185	0.020	0.170	0.150
	0.25g	0.095	0.309	0.285	0.075	0.275	0.250
MOD4	0.07g	0.060	0.075	0.058	0.020	0.020	0.018
	0.15g	0.085	0.110	0.070	0.050	0.080	0.022
	0.25g	0.100	0.198	0.195	0.100	0.158	0.160

pressure distribution due to dynamic loading (fig.16c) for the said input motion. From the excess pore water pressure variation plot, it is quite evident that, maximum excess pore pressure is observed in the soft foundation clayey soil layer.

The excess pore pressure results in a reduction of effective stress that causes the instability in the embankment. Excess pore pressure ratio is an indicator of the actual instability in any portion of the model. In the Fig. 17, the excess pore pressure ratio contour of MOD1 for input PGA 0.25g, 0.15g, 0.07g after application of dynamic loading is shown. The maximum generation of excess pore pressure ratio is restricted mainly in soft clay layer and this maximum value of excess pore pressure ratio increases with PGA of input motion. The excess pore pressure ratio is defined as the ratio of pore water pressure in excess to the original pore water pressure at an instant to the initial effective stress.

Figure 18 presents the similar pore pressure ratio contour for MOD4 at the end of the seismic loading. For better understanding and to get more clear insight about the variation, the variation of excess pore pressure ratio with dynamic loading period has also been plotted. The variations have been plotted for different locations within the soft foundation soil layer.

Figure 16.
Pore Pressure Contours in different stages of loading (MOD1; PGA: 0.25g): (a) Before dynamic loading, (b) after dynamic loading and (c) Excess pore pressure distribution

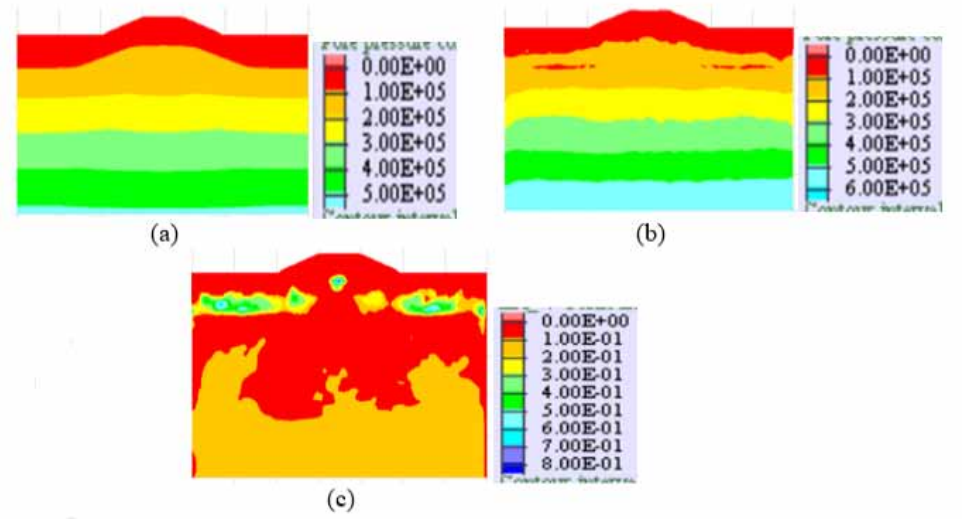

Figure 17.
Contour of Excess Pore Pressure Ratio for MOD1 under damped condition for PGA: (a) 0.07g, (b) 0.15g and (c) 0.25g

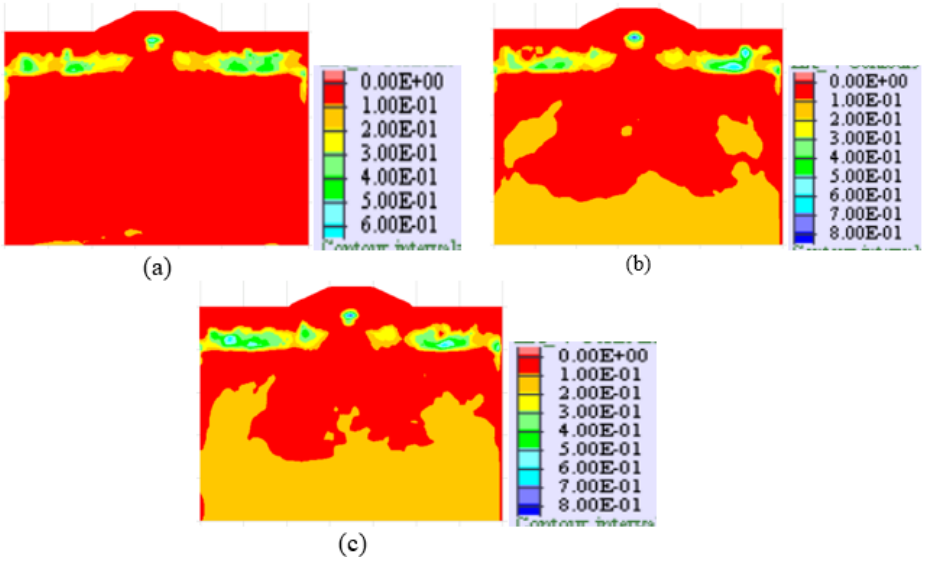

Figure 18.
Contour of Excess Pore Pressure Ratio for MOD4 under damped condition for PGA: (a) 0.07g, (b) 0.15g and (c) 0.25g

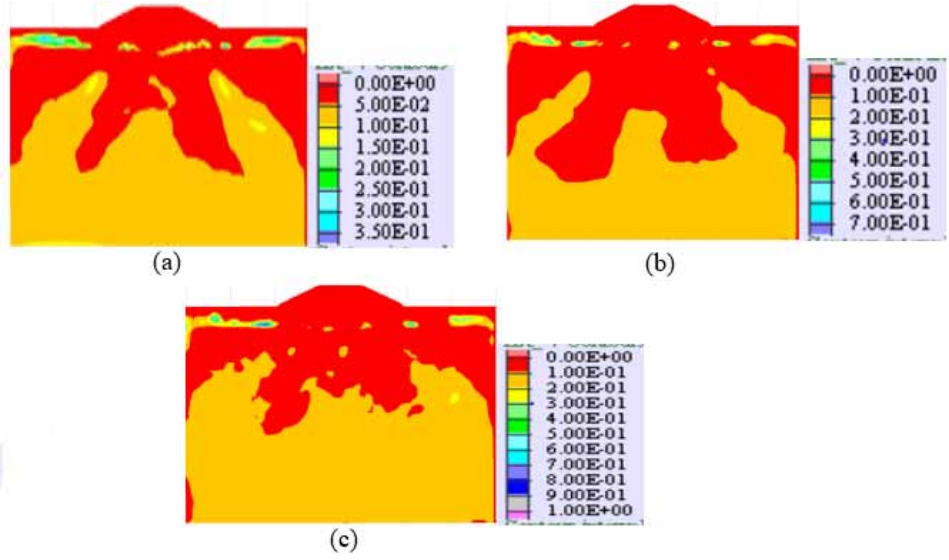

Figures 19 and 20 show the excess pore pressure history with dynamic time at different locations of MOD1 and MOD4, respectively, along with for different input ground motions. It can be observed that at different locations, the excess pore pressure histories are very different and it further depends on the PGA of the input motion and thickness of the soft soil layer. Though in several cases the maximum momentary excess pore pressure ratio attains maximum values more than 1, but the sustained pore pressure ratio at the end of dynamic loading time is quiet low and well below 1. From the figures, it

Figure 19.
Excess pore pressure ratio vs Dynamic Time under damped condition (MOD1) for PGA: (a) 0.07g, (b) 0.15g and (c) 0.25g

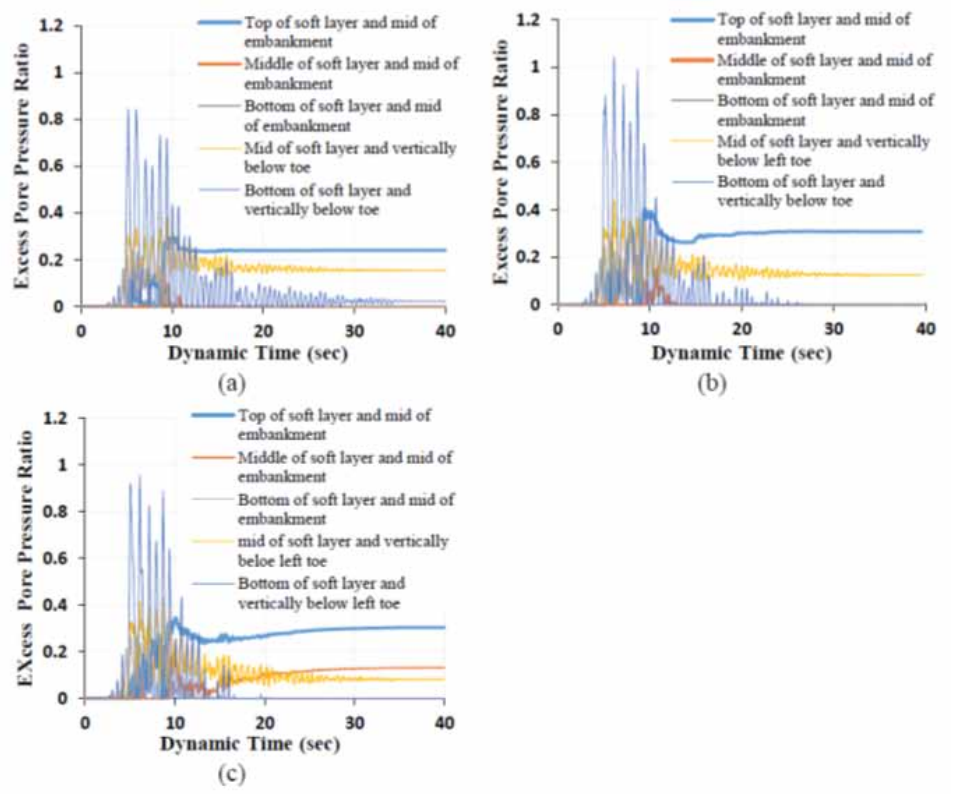

can be observed that the bottom of embankment (or top of soft layer) shows maximum excess pore pressure ratio generation under all three input motions with a soft layer thickness of 10m (Fig. 19). The MOD4 with soft layer thickness of 5m doesn't exhibit any such sustained pore pressure at the end of dynamic loading. So, lesser thickness of soft soil layer may not exhibit any such sustained excess pore pressure ratio at the end of dynamic loading except few spikes.

4. CONCLUSION

The study presents the characteristic responses of a low height embankment, typically used for road embankment, constructed on soft clay under seismic loading. In addition to that, the variations in soft layer thickness, shaking intensity and velocity of stiffer soil layer have also been studied.

1. All the considered models exhibit static factor of safety greater than 1.50 which signifies quite stable slopes and potential slope-failure mode is base failure. For both the thicknesses of soft foundation soil layer, the potential failure surface is restricted up to the soft layer only. The static FOS increases from 1.67 to 1.80 as the thickness of soft soil layer decreases from 10m to 5m.
2. The PGA amplification between the base and embankment top ($a_{max,crest}$ / $a_{max,base}$) is studied for all the considered cases. Amplification is found highest for the lowest input PGA, i.e., 0.07g, and the amplification is lowest for the highest input PGA, i.e., 0.25g. The PGA amplification for 0.07g input motion lies in the range of 2.8 to 3.3, for 0.25g input motion the amplification

Figure 20.
Excess pore pressure ratio vs Dynamic Time under damped condition (MOD4) for PGA: (a) 0.07g, (b) 0.15g and (c) 0.25g

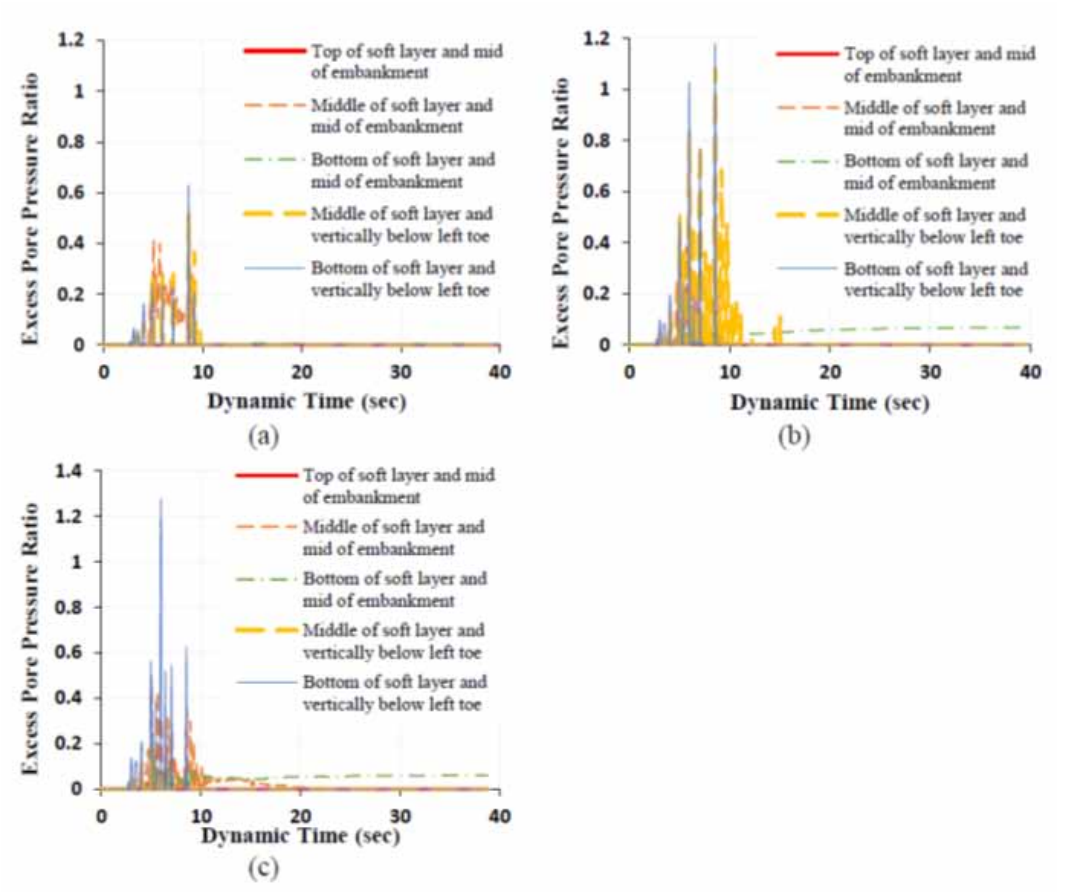

ranges from 1.15 to 1.25 and for 0.15g input motion the amplification lies in the range of 1.65 to 1.9 among all the considered cases.

3. The vertical settlements at crest are found to be influenced by the thickness of the soft soil layer below the embankment and by the PGA of the input motion. In most of the cases, the damped vertical crest settlement is greater than the undamped vertical crest settlement due to the decrease of shear modulus with accumulated permanent strain in case of damped settlement except few cases in the lower PGA range (PGA 0.07g) due to the fact that the greater acceleration amplification in undamped case is more dominant than the shear modulus degradation in damped case. The maximum vertical crest settlement varies from ~100mm to 250mm in case of 10m soft soil thickness, whereas, 30mm to 70mm for 5m soft layer thickness among all the considered cases.
4. In the soft layer, a significant amount of horizontal displacement is observed. For all the considered cases, the horizontal displacement is small in the central region of the whole embankment but with the increase in distance away from the middle of the embankment, the horizontal displacement increases. With the increase in input motion PGA and soft layer thickness, the horizontal displacement is found to increase. The maximum horizontal displacement occurs in the toe region for all the considered cases. Final permanent horizontal displacement in the

middle of the soft layer varies from ~85mm to 275mm (MOD1) for 10m thickness of soft layer, whereas, ~20mm to 160mm (MOD4) for 5m thickness of soft layer.

5. With the application of seismic input motion, the excess pore pressure gets generated within the saturated zone of the model. The generation of the excess pore pressure depends on the intensity of shaking along with the thickness of soft soil layer. It is observed that the bottom of embankment (or top of soft layer; section through the middle) shows maximum excess pore pressure ratio under all the three considered input motions with a soft layer thickness of 10m. A sustained little excess pore pressure ratio at the end of the dynamic loading is also observed. The maximum value of this sustained excess pore pressure ratio is found well below 0.5. No such (or negligible) sustained pore pressure ratio is observed for 5m soft soil layer thickness.

COMPETING INTERESTS

All authors of this article declare there are no competing interests.

FUNDING AGENCY

This research received no specific grant from any funding agency in the public, commercial, or not-for-profit sectors. Funding for this research was covered by the author(s) of the article.

DATA AVAILABILITY

The datasets generated during and/or analysed during the current study are available from the corresponding author on reasonable request.

AUTHORS' CONTRIBUTIONS

Debabrata Ghosh: Conception and design of study, numerical simulation, analysis and/or interpretation of data, drafting the manuscript

Narayan Roy; Manuscript editing & revising the manuscript critically for important intellectual content.

Ramendu Bikas Sahu: Supervision of the work carried out & revising the manuscript critically for important intellectual content.

REFERENCES

Bandopadhyay, S., Banerjee, R., Sengupta, S., Parulekar, Y. M., & Reddy, G. Rami. (2017). A Comparative Assessment of the Seismic Response of an Earthen Dam Using Analytical Simulation and Empirical Methods. Current science, 113(5). doi:10.18520/cs/v113/i05/902-910

Bardhan, A., & Samui, P. (2022). Application of Artificial Intelligence Techniques in Slope Stability Analysis: A Short Review and Future Prospects. *International Journal of Geotechnical Earthquake Engineering*, *13*(1), 1–22. doi:10.4018/IJGEE.298988

Cappa, R., Yniesta, S., Brandenberg, S. J., & Lemnitzer, A. (2015). *Settlements and excess pore pressure generation in peaty soils under embankments during cyclic loading*. 6th International Conference on Earthquake Geotechnical Engineering,Christchurch, *New Zealand.*

Chopra, A. K. (1966). Earthquake effects on dams. [Ph.D. dissertation, University of California, USA].

Egawa, T., Nishimoto, S., & Tomisawa, K. (2004). An Experimental Study on the Seismic Behavior of Embankments on Peaty Soft Ground through Centrifuge Model Tests. *13th World Conference on Earthquake Engineering Vancouver, B.C.*, Canada Paper No. 36.

Giri, D., & Sengupta, A. (2010). *Performance of Small-Scale Model Slopes in Shaking Table Tests.* Indian Geotechnical Conference, GEOtrendz. IGS Mumbai Chapter & IIT Bombay.

Gordan, B., Adnan,A., & Aida, A.K.M. (2014). Soil Saturated Simulation in Embankment during Strong Earthquake by Effect of Elasticity Modulus. *Hindawi Publishing Corporation; Modelling and Simulation in Engineering, 2014, Article ID 191460,* 7 pages. 10.1155/2014/191460

Jakka, R. S., Ramana, G. V., & Datta, M. (2011). Seismic Slope Stability of Embankments Constructed with Pond Ash. *Seismic Slope Stability of Embankments Constructed with Pond Ash.*, *29*(5), 821–835. doi:10.1007/s10706-011-9419-8

Lefebvre, G., & Pfendler, P. (1996). Strain Rate and Preshear Effects in Cyclic Resistance of Soft Clay. *Journal of Geotechnical Engineering*, *122*(1), 21–26. doi:10.1061/(ASCE)0733-9410(1996)122:1(21)

Long, X., & Tjok, K. M. (2013). Analyses of Seismic Slope Stability and Subsequent Debris Flow Modeling. *Fugro GeoConsutling Inc., Houston, T*, *Proceedings of the 18th International Conference on Soil Mechanics and Geotechnical Engineering*, Paris.

Makdisi, F., & Seed, H. (1978). Simplified procedure for estimating dam and embankment earthquake induced deformations. *Journal of the Geotechnical Engineering Division*, *104*(7), 849–867. doi:10.1061/AJGEB6.0000668

Melo, C., & Sharma, S. (2004). Seismic Coefficients for Pseudostatic Slope Analysis. *13th World Conference on Earthquake Engineering,* Vancouver, B.C., Canada. Paper No. 369.

Newmark, N. M. (1965). Effects of earthquakes on dams and embankment. *Geotechnique*, *15*(2), 139–160. doi:10.1680/geot.1965.15.2.139

Okamura, M., & Tamamura, S. (2011). Seismic stability of embankment on soft soil deposit. *International Journal of Physical Modelling in Geotechnics*, *11*(2), 50–57. doi:10.1680/ijpmg.2011.11.2.50

Parish, Y., Sadek, M., & Shahrour, I. (2009). Review Article: Numerical analysis of the seismic behaviour of earth dam. *Natural Hazards and Earth System Sciences*, *9*(2), 451–458. doi:10.5194/nhess-9-451-2009

Rahardjo, P. P. (2014). Geotechnical Failures Case Histories of Construction on Soft Soils, Forensic Investigations and Counter Measures in Indonesia. *International Journal of Integrated Engineering*, *6*(2), 11–23.

Seed, H. B., Lee, K. L., Idriss, I. M., & Makdisi, R. (1973). *Analysis of the slides in the San Fernando dams during the earthquake of Feb 9,1971. Report No. EERC 73-2*. Earthquake Engineering Research Centre, University of California.

Singh, R., & Roy, D. (2009). Estimation of earthquake-induced crest settlements of embankments. *American Journal of Engineering and Applied Sciences*, *2*(3), 515–525. doi:10.3844/ajeassp.2009.515.525

Sitharam, T. G., & Hegde, A. M. (2019). A Case Study of Probabilistic Seismic Slope Stability Analysis of Rock Fill Tailing Dam. *International Journal of Geotechnical Earthquake Engineering*, *10*(1), 43–60. doi:10.4018/IJGEE.2019010104

Terzaghi, K. (1950). Mechanisms of Landslides. *Engineering Geology (Berkeley) Volume*. *Geological Society of America*, *1950*. doi:10.1061/(ASCE)0733-9410(1996)122:1(21)

Wartman, J., Bray, J. D., & Seed, R. B. (2001). Shaking Table Experiment of a Model Slope Subjected to a Pair of Repeated Ground Motions. *Fourth International conference on recent advances in geotechnical earthquake engineering and soil dynamics*, Missouri University of science & technology, USA.

Yu-liang, L., Feng, S., Xiao, Y., Guo-lin, Y., & Li-min, L. (2016). Numerical analysis on seismic behavior of railway earth embankment: A case study. *Journal of Central South University*, *2016*(23), 906–918. doi:10.1007/s11771-016-3138-5

Zhai, E., Roth, W., Dawson, E., & Davis, C. (2004). Seismic deformation analysis of an earth dam - a comparison study between equivalent-linear and nonlinear effective-stress approaches. *13th World Conference on Earthquake Engineering, Vancouver, B.C., Canada*, Paper No. 3298.